Determination of Sulfadiazine in Natural Waters by Pine Needle Biochar – Derivatized Magnetic Nanocomposite Based Solid-Phase Extraction (SPE) with High-Performance Liquid Chromatography (HPLC)

Remziye Nur Avcı, Tülay Oymak & Esra Bağda

Taylor & Francis
Taylor & Francis Group

LIQUID CHROMATOGRAPHY

Check for updates

Determination of Sulfadiazine in Natural Waters by Pine Needle Biochar – Derivatized Magnetic Nanocomposite Based Solid-Phase Extraction (SPE) with High-Performance Liquid Chromatography (HPLC)

Remziye Nur Avcı, Tülay Oymak, and Esra Bağda

Department of Basic Pharmaceutical Sciences, Analytical Chemistry Division, Faculty of Pharmacy, Sivas Cumhuriyet University, Sivas, Turkey

ABSTRACT

A magnetic solid-phase extraction (MSPE) method was developed for the facile and sensitive determination of sulfadiazine prior to high-performance liquid chromatography (HPLC) analysis. The magnetic sorbent was prepared by the chemical co-precipitation of Fe_3O_4 magnetic nanocomposites modified with biochar. Characterization of the synthesized Fe_3O_4@BC-PN (Fe_3O_4 loaded pine leaves derived biochar) was performed by scanning electron microscopy – energy dispersive x-ray spectrometry (SEM-EDS), X-ray diffraction (XRD), vibrating sample magnetometry (VSM), and Brunauer – Emmett – Teller (BET) surface analysis. The saturation magnetization value was 17.95 emu/g by vibrating sample magnetometry. The Fe_3O_4@BC-PN particle sizes were determined to be 11.8 nm using the Debye-Scherrer relationship. The pH, mass of adsorbent, type, and volume of eluent were optimized. The limits of detection and quantification of the developed MSPE HPLC method were 10.7 μg/L and 35.5 μg/L, respectively. The intra-day and inter-day repeatabilities were below 4.2% and 7.7%, respectively. The developed method was employed to determine trace levels of sulfadiazine in spiked water samples.

Introduction

Antibiotics are frequently used to treat infectious diseases. The use of antibiotics has steadily increased worldwide (Kraemer, Ramachandran, and Perron 2019). van Boeckel et al. (2015) stated that the antibiotic consumption in livestock reached 63,151 tons in 2010 and is predicted to increase by 67% by 2030 and nearly double in Brazil, Russia, India, China, and South Africa. The stability of antibiotics under environmental conditions cause antibiotic resistance (Baby et al. 2021). Monitoring the accumulation and concentration of antibiotics in environmental samples is essential for developing protection strategies. Sulfadiazine (SDZ) is a sulfonamide that has been approved by the United States Food and Drug Administration to treat certain types of infectious diseases

and is widely used for prophylaxis and therapeutics of diseases in land and aquatic animals (Kokulnathan et al. 2021; Xu et al. 2021). The studies show that sulfonamides may be present in soil for long periods (Schauss et al. 2009).

Determining sulfadiazine levels in environmental samples with new analytical methods is essential for preventing antibiotic pollution and developing ecological strategies. Various methods for the determination of sulfadiazine are available in the literature. However, developing rapid, simple, environmentally friendly, and green analytical detection techniques is a critical topic. In a literature survey with the keywords 'determination of sulfadiazine' in the Web of Science database, 511 studies were obtained (access date 10.01.2022). 490 of these studies are research articles, with 34 published in 2017 and 32 in 2021. Thus, there is an increasing need for determining the concentration of sulfadiazine. Surprisingly, few studies have systematically evaluated the use of magnetic biochar for magnetic solid-phase extraction (MSPE) of sulfadiazine. In recent years, biochars have become attractive as adsorbents due to their low cost, environmental friendliness, high thermal stability, porous structure, large surface area, large pore volumes, and the presence of functional groups. Suitable biomass for the production of biochar is an important consideration because the quality and cost depend on the raw material (Rangabhashiyam and Balasubramanian 2019; Nicolaou et al. 2019) . However, the separation of biochar from the aqueous solution is an important problem in adsorption studies. In addition, desorption of adsorbed species may occur, leading to secondary pollution, low recovery, and time consuming. To solve this problem, loading magnetic material into biochar is an effective strategy because of the simple removal from aqueous media by magnetic separation. In particular, magnetic biochar, which has the combined properties of biochar and magnetic material, is suitable for adsorption studies (El-Azazy et al. 2020; Gu, Xue, and Zhang 2021; Yi et al. 2020; Zhao et al. 2021).

In the present study, a simple magnetic solid-phase extraction method was developed to rapidly extract and preconcentrate sulfadiazine from water samples prior to HPLC analysis. Fe_3O_4 magnetic nanocomposites modified with biochar obtained from pine needles as the sorbent was synthesized by chemical co-precipitation and characterized and demonstrated to be useful for MSPE of trace levels of sulfadiazine in various water samples. The developed method is simple, easy to apply, and environmentally friendly and the sorbent was synthesized using widely available materials.

Materials and methods

All reagents were of analytical grade and used without further purification. All solutions were prepared in deionized water (18.2 MΩ). Sulfadiazine, HCl, CH_3COOH, H_3PO_4, and NH_3 were purchased from Sigma Aldrich; KCl, KH_2PO_4, and acetonitrile were from Carlo Erba; and K_2HPO_4 from Scharlau Chemical. 10 mg of sulfadiazine were dissolved in 50 mL of 0.010 M NaOH to obtain 100 mg/L sulfadiazine. The appropriate volumes of 1.0 M of KH_2PO_4, 1.0 M of K_2HPO_4, and 1.0 M of H_3PO_4 were mixed to prepare buffer solutions. 70.0 mL of formic acid (0.1%) and 30.0 mL of acetonitrile were mixed, degassed, and used as the mobile phase for HPLC. Sulfadiazine calibration solutions were prepared in 5% NH_3-methanol to ensure matrix matching of the sample

solutions with calibration solutions. 5 mL of stock NH_3 (26%) were diluted to 100 mL with methanol to obtain 5% NH_3-methanol.

Crystal structure analysis of magnetic solid nanocomposite was determined with X-ray diffraction (XRD) (Pan Analytical, Cu K_α radiation at 0.15 nm). Scanning electron microscopy – energy dispersive x-ray spectrometry (SEM-EDS) was conducted with a Tesca MIRA3 instrument. SEM was used for topographic imaging and EDS to characterize the elemental composition of the biochars. Brunauer-Emmett-Teller (BET) analyses were done with a Quantachrome, Nova Touch LX4 instrument at 77 K with liquid N_2. The magnetic properties of nanocomposite were determined by a Lake Shore 7407 vibrating sample magnetometer (VSM).

Preparation of magnetic nanocomposite

The preparation of magnetic nanocomposite was performed according to literature with modifications (El-Sheikh, Nofal, and Shtaiwi 2019; He et al. 2019; Yang et al. 2013; You et al. 2019). The pine needles were collected and washed with deionized water to remove dust, dried at 60 °C, and ground to small pieces. To obtain the biochar, the ground material was heated to 1000 °C for 2 hours.

2.0 g of biochar were added to 200 mL of deionized water and sonicated to obtain a finely dispersed solution. 6.1 g of $FeCl_3·6H_2O$ were dissolved in 100 mL of deionized water, and 4.2 g of $FeSO_4·7H_2O$ and a few drops of concentrated HCl were added. The solution was heated to 90 °C, and 20 mL of NH_3 and dispersed biochar solution were added. The mixture was incubated for 30 minutes at 90 °C and the magnetic nanocomposite material was separated from the aqueous phase with a magnet. The material was washed with water and ethanol several times and dried at 60 °C.

Separation and preconcentration of sulfadiazine by magnetic solid-phase extraction

Firstly, 150 mg of Fe_3O_4@BC-PN powder were washed with deionized water and the buffer solution. The material was mixed with 40 mL of 0.5 mg L^{-1} of sulfadiazine solution buffered to pH 7.0 at 50 rpm for 10 minutes, the Fe_3O_4@BC-PN powder was held with a magnet, and the aqueous phase was decanted. 1.0 mL of 5% NH_3-methanol was added to the Fe_3O_4@BC-PN powder and the tube was tightly closed. The mixture was vortexed for 10 minutes at 1000 rpm to achieve complete elution. Lastly, the Fe_3O_4@BC-PN powder was removed, and 20 μL of the NH_3-methanol phase was analyzed by HPLC.

A ProntoSILC18 ace -EPS (250 × 4.6 mm, 4 μm) column was used for chromatographic separation. The mobile phase composed of 70% formic acid (0.1%) and 30% acetonitrile was used in an isocratic mode. The mobile phase flow rate was adjusted to 1 mL/min, the detection wavelength was 270 nm, and the sample injection volume was 20 μL.

Results and discussion

Characterization results

The evaluation of SEM images and EDS measurements is essential for evaluating elemental composition and topological data and is frequently used to characterize magnetic materials
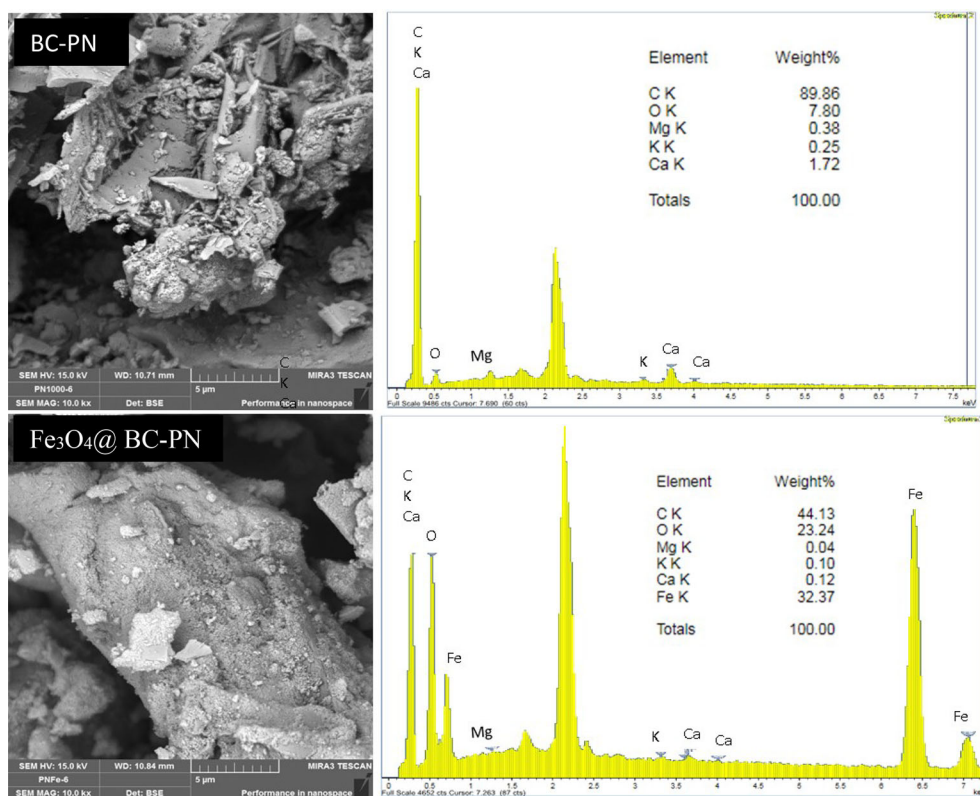
Figure 1. Scanning electron micrographs and energy dispersive x-ray spectra of pine needles derived biochar (BC-PN) and Fe_3O_4 loaded pine needles derived biochar (Fe_3O_4@BC-PN).

(Jack et al. 2019). The SEM images and EDS spectra of BC-PN and Fe_3O_4@BC-PN are shown in Figure 1. The surface topologies of BC-PN and Fe_3O_4@BC-PN nanocomposite are different. After the modification, the iron oxide particles were embedded in the BC-PN. The EDS spectrum of BC-PN shows that BC-PN contains Ca, Mg, and K in addition to C and O. On the other hand, the EDS spectrum of Fe_3O_4@BC-PN shows the presence of Fe and BC-PN. The elemental carbon percentage was 90% for BC-PN and 44% for Fe_3O_4@BC-PN. In addition, approximately 32% of the elemental composition is iron for Fe_3O_4@BC-PN, indicating that the magnetic nanocomposite was synthesized (Quah et al. 2020; Salimi et al. 2019; Shang et al. 2016; Yan et al. 2015).

The surface area, pore volume, and pore diameter of a material used for solid-phase extraction affect the extraction efficiency and time and must be determined. An increase in the surface area generally enhances the interaction area, which substantially improves the extraction efficiency.

The textural characteristics of bare BC-PN and Fe_3O_4@BC-PN were investigated by the Brunauer-Emmett-Teller method. The results are provided in Table 1 and show that the surface area of Fe_3O_4@BC-PN is higher than for the bare BC-PN. El-Azazy et al. (2020) reported that the higher surface area of Fe_3O_4@BC-PN may be due to magnetite nanoparticles on the biochar surface. Similar observations were also provided by Mahanty and Mondal (2021). They indicated the surface area of biochar increased after magnetization

Table 1. Brunauer-Emmett-Teller surface area, average pore volume, and average pore radius of the synthesized materials.

	BET surface area, $m^2 g^{-1}$	Average pore volume, $cm^3 \cdot g^{-1}$	Average pore radius, angstroms
BC-PN	75.5	0.05	18.9
Fe_3O_4	85.3	0.29	57.8
Fe_3O_4@BC-PN	93.8	0.196	67.5

BET: Brunauer-Emmett-Teller, BC-PN: pine needles derived biochar; Fe_3O_4@BC-PN: Fe_3O_4 loaded pine needles derived biochar.
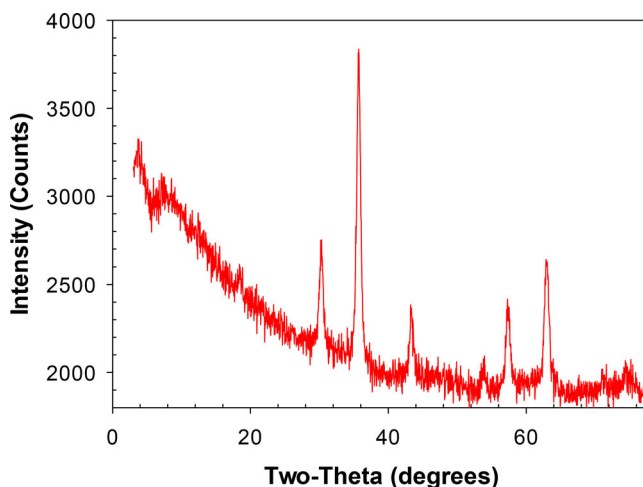
Figure 2. X-ray diffraction pattern for Fe_3O_4 loaded pine needles derived biochar (Fe_3O_4@BC-PN).

with iron oxides from 16.48 to 183.62 m^2/g. The specific surface area of Fe_3O_4@BC-PN was similar to that of bagasse magnetic biochar synthesized by Liang et al. (2020). The surface area of Fe_3O_4@BC-PN was approximately 40 times the specific surface area of rice straw and 27 times the specific surface area of the material synthesized by Tan et al. (2017). The average pore volume and pore radius were also higher for Fe_3O_4@BC-PN.

The x-ray diffraction pattern of Fe_3O_4@BC-PN is shown in Figure 2. The characteristic peaks of the synthesized Fe_3O_4@BC-PN at 30.3°, 35.7°, 43.3°, 54.1°, 57.3°, and 62.9° are assigned to the indexed planes (220), (311), (400), (422), (511), and (440). These match the pattern of Fe_3O_4 (magnetite) (Keshavarz and Ghasemi 2011; El-Sheikh, Nofal, and Shtaiwi 2019; El Ghandoor et al. 2012; Noriega-Luna et al. 2014; Pant et al. 1995; Yang et al. 2020).

The crystal size was determined using the Debye–Scherrer equation (Aguiar et al. 2018; El Ghandoor et al. 2012): $\tau = k\lambda/B\cos\theta$ where k is 0.9, λ is the wavelength of the incident radiation (0.154056 nm), θ is the Bragg angle, and B is the full width at half maximum (FWHM) of the peak. The particle size of Fe_3O_4@BC-PN was determined to be 11.8 nm using the most intense peak with 2θ equal to 35.7°.

The use of magnetic materials as adsorbents allows rapid and easy separation. The magnetic properties of the Fe_3O_4@BC-PN were characterized at 288 K by applying a 20 kOe magnetic field. The magnetic hysteresis curve of Fe_3O_4@BC-PN is presented in Figure 3 and indicates that Fe_3O_4@BC-PN has superparamagnetic properties. The saturation magnetization of Fe_3O_4@BC-PN was 17.95 emu/g. Fe_3O_4 retained its magnetic

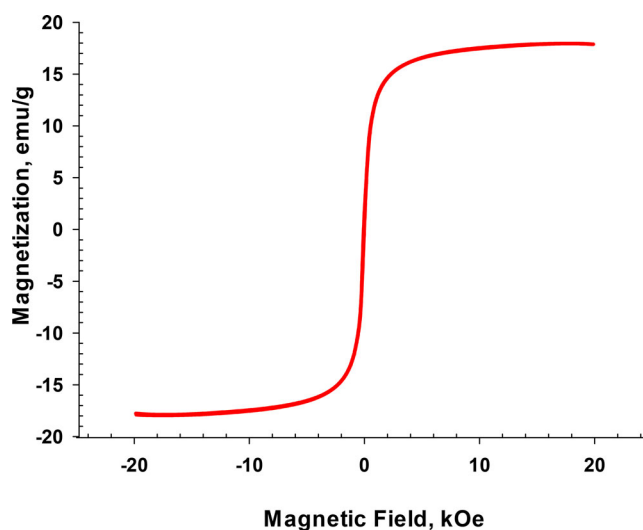**Figure 3.** Magnetic hysteresis curve of Fe$_3$O$_4$ loaded pine needles derived biochar (Fe$_3$O$_4$@BC-PN).

properties after modification which allows easy and rapid separation by a strong external magnetic field (Zheng et al. 2020).

Optimization of experimental parameters affecting the solid-phase extraction efficiency of sulfadiazine

The pH of the medium and mass of adsorbent affect the extraction efficiency of the analyte in solid-phase extraction. Therefore, these parameters were optimized to increase the extraction efficiency.

Influence of pH

The pH is critical for extraction as it influences the stability of the adsorbent, the charges on its surface, and charges of analytes (Sajid, Nazal, and Ihsanullah 2021). 25 mL model solutions containing 0.5 µg/mL sulfadiazine with 100 mg Fe$_3$O$_4$@BC-PN were prepared. The pH of the solutions was adjusted between 3.0 and 8.0 using buffer solutions as shown in Figure 4a. Increasing the pH from 3.0 to 4.0 increased the extraction efficiency from 72% to 82%. Between pH 6.0 and 8.0, the recovery reached its highest value, between 85 and 87%. Hence, a pH of 7 was employed in subsequent measurements.

The point of zero charge of Fe$_3$O$_4$@BC-PN is essential for elucidating the interaction mechanism. At pH lower than the pH$_{zpc}$, the positive charge density increases, while at higher pH, the negative charge density on the surface increases. The isoelectric point (pH$_{zpc}$) for Fe$_3$O$_4$@BC-PN was determined to be 5.6 (Figure 4b). In the acidic region, the positive charges dominate the surface. As the pH value approaches 5.6, the densities of positive and negative charges on the surface equalize. On the other hand, the pK$_{a1}$ and pK$_{a2}$ values of sulfadiazine are 1.57 and 6.50, illustrating its ampholytic properties (Sukul et al. 2008). The fraction of the neutral state of the sulfadiazine is high when the pH of the
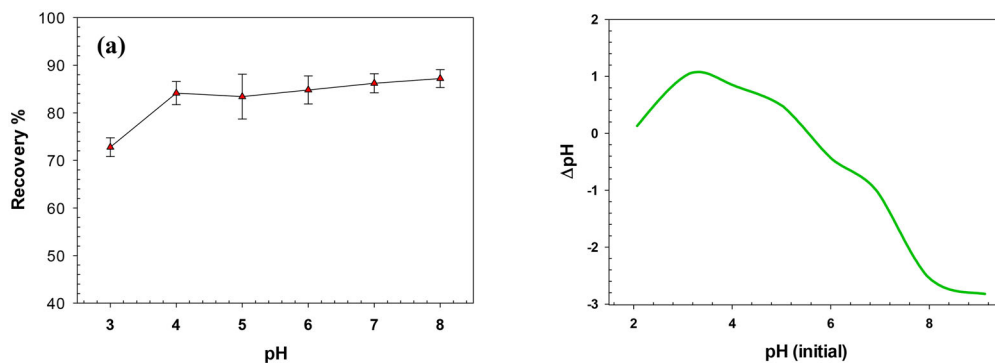
Figure 4. (a) Influence of pH on MSPE using 25 mL model solutions containing 0.5 mg/L sulfadiazine shaken at 50 rpm for 10 min. **(b)** Point of zero charge of Fe_3O_4 loaded pine needles derived biochar (Fe_3O_4@BC-PN).

solution is between these pK_a values. Sulfadiazine is in the cationic form in the acidic region. When pH exceeds 5, sulfadiazine is deprotonated and negatively charged (Di et al. 2020). The results show that the magnetic sorbent effectively adsorbs the neutral and anionic form of sulfadiazine. The material surface is also negatively charged at these pH values, so the interaction cannot be expected to be electrostatic attraction. Hence H-bonding, $\pi - \pi$ bonds, and hydrophobic interactions are more likely (Dutt et al. 2020). Since the biochar is prepared at high temperatures, the density of functional groups is not expected to be high. Therefore, the probability of hydrogen bonding interactions is low. As reported in the literature, hydrophobic effects (HPO) and $\pi - \pi$ electron donor $-$ acceptor (EDA) interactions between carbonaceous sorbents (e.g., biochar) and aromatic compounds (e.g., sulfadiazine) are possible mechanisms (Ling et al. 2016; Xiao and Pignatello 2015). Similar results have been reported in the literature. Dil et al. (2021) obtained the highest extraction capacity at pH 6 to enrich sulfadiazine and sulfathiazole from milk using syringe–to–syringe magnetic solid-phase microextraction.

Influence of the mass of Fe$_3$O$_4$@BC-PN

The mass of Fe_3O_4@BC-PN is critical to the extraction efficiency. To determine the optimum mass of adsorbent for the recovery of sulfadiazine, 50, 100, and 150 mg Fe_3O_4@BC-PN were added to 25 mL model solutions containing 0.5 mg/L sulfadiazine. The pH was adjusted to 7, followed by shaking at 50 rpm for 10 min. For 50 mg, 100 mg, and 150 mg of Fe_3O_4@BC-PN were used, the recoveries were $87.7 \pm 2.5\%$, $90.0 \pm 2.0\%$ and $95.1 \pm 2.1\%$, respectively (Table 2). The optimum mass of Fe_3O_4@BC-PN was 150 mg that was used in further measurements.

Influence of eluent

To examine the influence of the eluent on MSPE of sulfadiazine by Fe_3O_4@BC-PN, 2.5 mL of 5% NH_3, methanol, 5% NH_3-methanol, and 10% NH_3-methanol were investigated. The results are shown in Figure 5. Quantitative recovery was only obtained with 5% NH_3-methanol ($95.2 \pm 2.1\%$) and hence was employed in subsequent experiments.

Table 2. Optimization of the mass of Fe$_3$O$_4$@BC-PN for the recovery of sulfadiazine.

Mass of Fe$_3$O$_4$@BC-PN (mg)	Recovery, %
50	87.7 ± 2.5
100	90.0 ± 2.0
150	95.2 ± 2.1
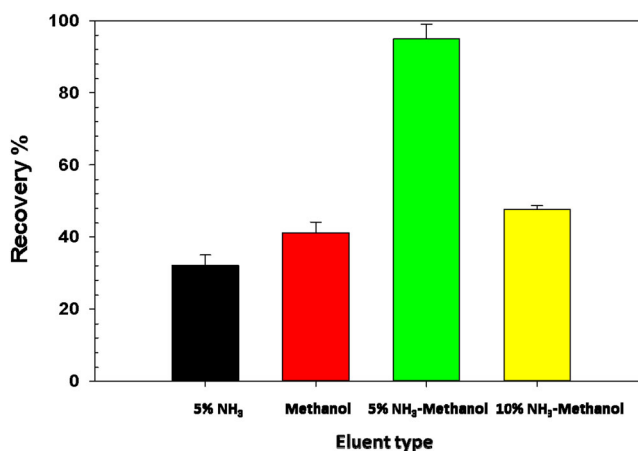
Figure 5. Influence of eluent using 25 mL model solutions containing 0.5 mg/L sulfadiazine at pH 7.0 with shaking at 50 rpm for 10 min.

Influence of sample volume and eluent volume

The sample and eluents volume are necessary for determining the enrichment factor. MSPE was applied to 25, 40, and 50 mL model solutions containing 150 mg adsorbent and 0.5 μg/mL sulfadiazine. The results are summarized in Table 3. The recovery of sulfadiazine was 96.2 ± 2.1% using the 40 mL sample volume.

MSPE method was performed with 1.0 mL and 2.5 mL of 5% NH$_3$-methanol as the eluent using the same conditions. The recovery was 95.1 ± 2.1% for 1.0 mL and 96.2 ± 2.1% for 2.5 mL. The enrichment factor was determined to be 40. The sample volume was deemed to be 40 mL and the eluent volume 1 mL for further work.

Analytical figures of merits for Fe$_3$O$_4$@BC-PN MSPE of sulfadiazine

To determine the limit of detection (LOD), 10 blank solutions containing 40 mL of 0.025 mg/L sulfadiazine were prepared. The developed MSPE method was applied to these solutions. The detection limit was obtained by dividing three times the standard deviation of the peak areas by the slope of the calibration line for the measurements of 10 blanks solutions containing 0.025 mg/L sulfadiazine. The detection limit was 10.7 μg/L considering the enrichment factor.

The limit of quantification (LOQ) was obtained by dividing ten times the standard deviation of the peak areas by the slope of the calibration line for the measurements of 10 solutions containing 0.025 mg/L sulfadiazine. The limit of quantification was 35.3 μg/L for sulfadiazine considering the enrichment factor.

Table 3. Influence of the sample volume upon the recovery of sulfadiazine.

Sample volume (mL)	Recovery, %
25	97.6 ± 1.5
40	96.2 ± 2.1 (for 2.5 mL eluent)
	95.1 ± 2.1 (for 1.0 mL eluent)
50	92.4 ± 3.3

Table 4. Intraday and inter-day reproducibilities of the developed magnetic solid-phase extraction method.

Added sulfadiazine (μg/mL)	Intra-day Repeatability		Inter-day Repeatability	
	Measured (μg/mL)	Relative standard deviation, %	Measured (μg/mL)	Relative standard deviation, %
0.05	0.046 ± 0.002	4.6	0.046 ± 0.004	7.7
0.2	0.20 ± 0.01	5.0	0.19 ± 0.01	5.2
0.5	0.48 ± 0.02	4.2	0.48 ± 0.01	2.1

Table 5. Application of proposed magnetic solid-phase extraction for the analysis of spiked water samples.

	River water	River water + 0.05 mg/L sulfadiazine	Tap water	Tap water + 0.05 mg/L sulfadiazine	Wastewater	Wastewater + 0.05 mg/L sulfadiazine
Recovery, %	–	85 ± 2	–	86.1 ± 2	–	52.5 ± 5

The intra-day and inter-day reproducibilities of Fe_3O_4@BC-PN MSPE were determined. Sulfadiazine solutions (0.05, 0.1, and 0.5 mg/L) were analyzed five times per day for three consecutive days. The averages, standard deviations, and relative standard deviations are provided in Table 4. The intra-day and inter-day reproducibilities of the method were reported as the relative standard deviations. The intra-day and inter-day reproducibilities for sulfadiazine were from 4.2 to 5.0% and 2.1 to 7.7%, respectively. The results show that the method has good reproducibility.

Adsorption capacity for sulfadiazine

The pH values of 40 mL model solutions containing 150 mg/L sulfadiazine were adjusted to 7 and added to tubes containing 150 mg Fe_3O_4@BC-PN. The system was mechanically shaken for 24 hours at room temperature (25 °C). The sulfadiazine concentrations (C_e) in the solution were determined. The adsorption capacity (q_e, mg/g) was determined by $q_e = (C_0 - C_e)V/m$ where C_0 and C_e are the initial and equilibrium concentrations of sulfadiazine, V is the solution volume, and m is the mass of Fe_3O_4@BC-PN. The adsorption capacity for SDZ was determined to be 7.9 mg/g.

Analysis of spiked water samples

The calibration curve for sulfadiazine was linear from 0.5 to 20 mg/L with a correlation coefficient of 0.999 (Figures S1 and S2) and described by $A = 94.1 \, C_{SDZ} - 24.4$ where

C_{SDZ} is the concentration of sulfadiazine in mg/L and A is the area of the chromatographic peak.

The developed Fe_3O_4@BC-PN MSPE method was employed to analyze wastewater, river water, and tap water for sulfadiazine. The samples were prepared as described above but without the addition of sulfadiazine and analyzed by HPLC. In addition, to characterize the accuracy, 0.05 mg/L sulfadiazine was added to each sample (Figures S3, S4, and S5) and the recoveries were determined (Table 5).

Conclusion

Antibiotic waste is a significant environmental problem due to the resistance to degradation and resulting persistence in the environment. Sulfadiazine, which is frequently used to treat infectious diseases, is widely used. Simple and sensitive methods are required to determine sulfadiazine in environmental samples. A new easily applicable MSPE approach was developed for the sensitive determination of trace sulfadiazine. The biocomposite prepared from biochar and nanocomposite material was characterized followed by characterization of the suitability for the determination of sulfadiazine. The parameters affecting the MSPE efficiency were optimized and the method was validated. The developed protocol was successfully applied to analyze spiked water samples.

Funding

References

Aguiar, H., S. Chiussi, M. López-Álvarez, P. González, and J. Serra. 2018. Structural characterization of bioceramics and mineralized tissues based on Raman and XRD techniques. *Ceramics International* 44 (1):495–504. doi:10.1016/j.ceramint.2017.09.203.

Baby, J. N., B. Sriram, S. F. Wang, and M. George. 2021. Integration of samarium vanadate/carbon nanofiber through synergy: An electrochemical tool for sulfadiazine analysis. *Journal of Hazardous Materials* 408:124940. doi:10.1016/j.jhazmat.2020.124940.

Di, S., J. Yu, P. Chen, G. Zhu, and S. Zhu. 2020. Net-like mesoporous carbon nanocomposites for magnetic solid-phase extraction of sulfonamides prior to their quantitation by UPLC-HRMS. *Microchimica Acta* 187 (2):1–11. doi:10.1007/s00604-019-4072-7.

Dil, E. A., M. Ghaedi, F. Mehrabi, and L. Tayebi. 2021. Highly selective magnetic dual template molecularly imprinted polymer for simultaneous enrichment of sulfadiazine and sulfathiazole from milk samples based on syringe-to-syringe magnetic solid-phase microextraction. *Talanta* 232:122449. doi:10.1016/j.talanta.2021.122449.

Dutt, M. A., M. A. Hanif, F. Nadeem, and H. N. Bhatti. 2020. A review of advances in engineered composite materials popular for wastewater treatment. *Journal of Environmental Chemical Engineering* 8 (5):104073. doi:10.1016/j.jece.2020.104073.

El Ghandoor, H., H. M. Zidan, M. M. Khalil, and M. I. M. Ismail. 2012. Synthesis and some physical properties of magnetite (Fe_3O_4) nanoparticles. *International Journal of Electrochemical Science* 7 (6):5734–45.

El-Azazy, M., A. S. El-Shafie, S. Al-Meer, and K. A. Al-Saad. 2020. Eco-Structured adsorptive removal of tigecycline from wastewater: Date pits' biochar versus the magnetic biochar. *Nanomaterials* 11 (1):30. doi:10.3390/nano11010030.

El-Sheikh, A. H., F. S. Nofal, and M. H. Shtaiwi. 2019. Adsorption and magnetic solid-phase extraction of cadmium and lead using magnetite modified with schiff bases. *Journal of Environmental Chemical Engineering* 7 (4):103229. doi:10.1016/j.jece.2019.103229.

Gu, Y., Y. Xue, and D. Zhang. 2021. Adsorption of aniline by magnetic biochar with high magnetic separation efficiency. *Environmental Pollutants and Bioavailability* 33 (1):66–75. doi:10.1080/26395940.2021.1920469.

He, C., J. Qu, Z. Yu, D. Chen, T. Su, L. He, Z. Zhao, C. Zhou, P. Hong, Y. Li, et al. 2019. Preparation of micro-nano material composed of oyster shell/Fe_3O_4 nanoparticles/humic acid and its application in selective removal of Hg (II). *Nanomaterials* 9 (7):953. doi:10.3390/nano9070953.

Jack, J., T. M. Huggins, Y. Huang, Y. Fang, and Z. J. Ren. 2019. Production of magnetic biochar from waste-derived fungal biomass for phosphorus removal and recovery. *Journal of Cleaner Production* 224:100–6. doi:10.1016/j.jclepro.2019.03.120.

Keshavarz, M, and Z. Z. Ghasemi. 2011. Coating of iron oxide nanoparticles with human and bovine serum albumins: A thermodynamic approach. *Journal of Physical & Theoretical Chemistry* 8 (2):7–17.

Kokulnathan, T., E. A. Kumar, T. J. Wang, and I. C. Cheng. 2021. Strontium tungstate-modified disposable strip for electrochemical detection of sulfadiazine in environmental samples. *Ecotoxicology and Environmental Safety* 208:111516. doi:10.1016/j.ecoenv.2020.111516.

Kraemer, S. A., A. Ramachandran, and G. G. Perron. 2019. Antibiotic pollution in the environment: From microbial ecology to public policy. *Microorganisms* 7 (6):180. doi:10.3390/microorganisms7060180.

Liang, M., Y. Ding, Q. Zhang, D. Wang, H. Li, and L. Lu. 2020. Removal of aqueous Cr (VI) by magnetic biochar derived from bagasse. *Scientific Reports* 10 (1):1–13. doi:10.1038/s41598-020-78142-3.

Ling, C., X. Li, Z. Zhang, F. Liu, Y. Deng, X. Zhang, A. Li, L. He, and B. Xing. 2016. High adsorption of sulfamethoxazole by an amine-modified Polystyrene-Divinylbenzene Resin and Its Mechanistic Insight. *Environmental Science & Technology* 50 (18):10015–23. doi:10.1021/acs.est.6b02846.

Mahanty, B., and S. Mondal. 2021. Synthesis of Magnetic Biochar Using Agricultural Waste for the Separation of Cr (VI) From Aqueous Solution. *Arabian Journal for Science and Engineering* 46 (11):10803–18. doi:10.1007/s13369-021-05572-0.

Nicolaou, E., K. Philippou, I. Anastopoulos, and I. Pashalidis. 2019. Copper adsorption by magnetized pine-needle biochar. *Processes* 7 (12):903–1000. doi:10.3390/pr7120903.

Noriega-Luna, B., L. A. Godíne, F. J. Rodríguez, A. Rodríguez, G. Zaldívar-Lelo De Larrea, C. F. Sosa-Ferreyra, R. F. Mercado-Curiel, J. Manríquez, and E. Bustos. 2014. Applications of dendrimers in drug delivery agents, diagnosis, therapy, and detection. *Journal of Nanomaterials* 2014:1–19. doi:10.1155/2014/507273.

Pant, R. P., R. M. Krishna, P. S. Negi, K. Ravat, U. Dhawan, S. K. Gupta, and D. K. Suri. 1995. XRD, SEM, EPR and microwave investigations of ferrofluid-PVA composite films. *Journal of Magnetism and Magnetic Materials* 149 (1–2):10–3. doi:10.1016/0304-8853(95)00318-5.

Quah, R. V., Y. H. Tan, N. M. Mubarak, J. Kansedo, M. Khalid, E. C. Abdullah, and M. O. Abdullah. 2020. Magnetic biochar derived from waste palm kernel shell for biodiesel production via sulfonation. *Waste Management (New York, NY)* 118:626–36. doi:10.1016/j.wasman.2020.09.016.

Rangabhashiyam, S., and P. Balasubramanian. 2019. The potential of lignocellulosic biomass precursors for biochar production: Performance, mechanism and wastewater application-a review. *Industrial Crops and Products* 128:405–23.

Sajid, M., M. K. Nazal, and I. Ihsanullah. 2021. Novel materials for dispersive (micro) solid-phase extraction of polycyclic aromatic hydrocarbons in environmental water samples: A review. *Analytica Chimica Acta* 1141:246–62. doi:10.1016/j.aca.2020.07.064.

Salimi, P., O. Norouzi, S. E. M. Pourhoseini, P. Bartocci, A. Tavasoli, D. Maria, S. M. Pirbazari, G. Bidini, and F. Fantozzi. 2019. Magnetic biochar obtained through catalytic pyrolysis of macroalgae: A promising anode material for Li-ion batteries. *Renewable Energy* 140:704–14. doi:10.1016/j.renene.2019.03.077.

Schauss, K., A. Focks, H. Heuer, A. Kotzerke, H. Schmitt, S. Thiele-Bruhn, K. Smalla, B. M. Wilke, M. Matthies, W. Amelung, et al. 2009. Analysis, fate and effects of the antibiotic sulfadiazine in soil ecosystems. *TrAC Trends in Analytical Chemistry* 28 (5):612–8. doi:10.1016/j.trac.2009.02.009.

Shang, J., J. Pi, M. Zong, Y. Wang, W. Li, and Q. Liao. 2016. Chromium removal using magnetic biochar derived from herb-residue. *Journal of the Taiwan Institute of Chemical Engineers* 68: 289–94. doi:10.1016/j.jtice.2016.09.012.

Sukul, P., M. Lamshöft, S. Zühlke, and M. Spiteller. 2008. Sorption and desorption of sulfadiazine in soil and soil-manure systems. *Chemosphere* 73 (8):1344–50. doi:10.1016/j.chemosphere.2008.06.066.

Tan, Z., Y. Wang, A. Kasiulienė, C. Huang, and P. Ai. 2017. Cadmium removal potential by rice straw-derived magnetic biochar. *Clean Technologies and Environmental Policy* 19 (3):761–74. doi:10.1007/s10098-016-1264-2.

van Boeckel, T. P., C. Brower, M. Gilbert, B. T. Grenfell, S. A. Levin, T. P. Robinson, A. Teillant, and R. Laxminarayan. 2015. Global trends in antimicrobial use in food animals. *Proceedings of the National Academy of Sciences of the United States of America* 112 (18):5649–54. doi:10.1073/pnas.1503141112.

Xiao, F., and J. J. Pignatello. 2015. π(+)-π interactions between (hetero)aromatic amine cations and the graphitic surfaces of pyrogenic carbonaceous materials. *Environmental Science & Technology* 49 (2):906–14. doi:10.1021/es5043029.

Xu, N., Y. Fu, F. Chen, Y. Liu, J. Dong, Y. Yang, S. Zhou, Q. Yang, and X. Ai. 2021. Sulfadiazine pharmacokinetics in grass carp (Ctenopharyngodon idellus) receiving oral and intravenous administrations. *Journal of Veterinary Pharmacology and Therapeutics* 44 (1):86–92. doi:10.1111/jvp.12918.

Yan, L., L. Kong, Z. Qu, L. Li, and G. Shen. 2015. Magnetic biochar decorated with ZnS nanocrytals for Pb (II) removal. *ACS Sustainable Chemistry & Engineering* 3 (1):125–32. doi:10.1021/sc500619r.

Yang, J., Q. Zeng, L. Peng, M. Lei, H. Song, B. Tie, and J. Gu. 2013. La-EDTA coated Fe_3O_4 nanomaterial: Preparation and application in removal of phosphate from water. *Journal of Environmental Sciences* 25 (2):413–8. doi:10.1016/S1001-0742(12)60014-X.

Yang, Y., G. Li, D. Wu, A. Wen, Y. Wu, and X. Zhou. 2020. β-Cyclodextrin-/AuNPs-functionalized covalent organic framework-based magnetic sorbent for solid phase extraction and determination of sulfonamides. *Microchimica Acta* 187 (5):1–10. doi:10.1007/s00604-020-04257-z.

Yi, Y., Z. Huang, B. Lu, J. Xian, E. P. Tsang, W. Cheng, J. Fang, and Z. Fang. 2020. Magnetic biochar for environmental remediation: A review. *Bioresource Technology* 298:122468–83. doi:10.1016/j.biortech.2019.122468.

You, Y., S. Zheng, H. Zang, F. Liu, F. Liu, and J. Liu. 2019. Stimulatory effect of magnetite on the syntrophic metabolism of Geobacter co-cultures: Influences of surface coating. *Geochimica et Cosmochimica Acta* 256:82–96. doi:10.1016/j.gca.2018.02.009.

Zhao, C., B. Wang, B. K. G. Theng, P. Wu, F. Liu, S. Wang, X. Lee, M. Chen, L. Li, and X. Zhang. 2021. Formation and mechanisms of nano-metal oxide-biochar composites for pollutants removal: A review. *The Science of the Total Environment* 767:145305. doi:10.1016/j.scitotenv.2021.145305.

Zheng, L., Y. Gao, J. Du, W. Zhang, Y. Huang, L. Wang, Q. Zhao, and X. Pan. 2020. A novel, recyclable magnetic biochar modified by chitosan–EDTA for the effective removal of Pb (II) from aqueous solution. *RSC Advances* 10 (66):40196–205. doi:10.1039/D0RA07499C.